Hindawi Publishing Corporation
International Journal of Photoenergy
Volume 2015, Article ID 982064, 8 pages
http://dx.doi.org/10.1155/2015/982064

Research Article

Enhanced Power Conversion Efficiency of P3HT : $PC_{71}BM$ Bulk Heterojunction Polymer Solar Cells by Doping a High-Mobility Small Organic Molecule

Hanyu Wang,[1] Xiao Wang,[1] Pu Fan,[1] Xin Yang,[2] and Junsheng Yu[1,2]

[1]*State Key Laboratory of Electronic Thin Films and Integrated Devices, School of Optoelectronic Information, University of Electronic Science and Technology of China (UESTC), Chengdu 610054, China*
[2]*Co-Innovation Center for Micro/Nano Optoelectronic Materials and Devices, Research Institute for New Materials and Technology, Chongqing University of Arts and Sciences, Chongqing 402160, China*

Correspondence should be addressed to Junsheng Yu; jsyu@uestc.edu.cn

Received 28 July 2015; Revised 9 September 2015; Accepted 9 September 2015

Academic Editor: Maria Vasilopoulou

The effect of molecular doping with TIPS-pentacene on the photovoltaic performance of polymer solar cells (PSCs) with a structure of ITO/ZnO/poly(3-hexylthiophene-2,5-diyl) (P3HT) : [6,6]-phenyl C71-butyric acid methyl ester ($PC_{71}BM$) : TIPS-pentacene/MoO_x/Ag was systematically investigated by adjusting TIPS-pentacene doping ratios ranged from 0.3 to 1.2 wt%. The device with 0.6 wt% TIPS-pentacene exhibited the enhanced short-circuit current and fill factor by 1.23 mA/cm^2 and 7.8%, respectively, resulting in a maximum power conversion efficiency of 4.13%, which is one-third higher than that of the undoped one. The photovoltaic performance improvement was mainly due to the balanced charge carrier mobility, enhanced crystallinity, and matched cascade energy level alignment in TIPS-pentacene doped active layer, resulting in the efficient charge separation, transport, and collection.

1. Introduction

Polymer solar cells (PSCs), as one of the most promising energy conversion technologies, have attracted much attention in last decades due to their unique properties of low cost, being easily manufactured, large scale, and being flexible [1–5]. The PSCs have many excellent applications, such as incorporation with wearable products, decoration of buildings, and space application for optimizing the design of space solar power. Recently, the power conversion efficiencies (PCEs) have reached 10% and 11% for the PSCs using single-junction and multijunction structures, respectively [6, 7]. However, the PCEs are still not high enough for commercialization. Therefore, great effort is devoted to further improve the photovoltaic performance of PSCs. The major drawbacks of PSCs are often attributed to low light absorption, limited exciton migration, and low hole transport ability [8]. Particularly, the low hole transport ability could increase the carrier recombination in the active layer and suppress the charge carrier collection [9]. Hence, a relatively low short-circuit current (J_{SC}) and fill factor (FF) are often observed in such PSCs.

In order to increase the hole transport ability of organic active layers, numerous approaches have been applied, such as modifying metal/semiconductor interface [10], introducing multisolvents [11], processing solvent additives [12], and doping a small amount of high-mobility materials [13]. Among them, molecular doping is an effective method to enhance hole transport ability of PSCs. For example, Liu et al. enhanced the PCE of PSCs by adding a high-mobility conjugated polymer with suitable energy band structure [13]. P-type molecular doping of F4-TCNQ improved the hole density and hole mobility in the polymer: fullerene derivative blends [14]. Pentacene, a high hole mobility small molecule used in organic thin-film transistors (OFETs), was successfully added in the poly(3-hexylthiophene-2,5-diyl) (P3HT) : [6,6]-phenyl C61-butyric acid methyl ester ($PC_{61}BM$) blends to balance hole and electron mobility and improve the photovoltaic performance of relative PSCs [15–17].

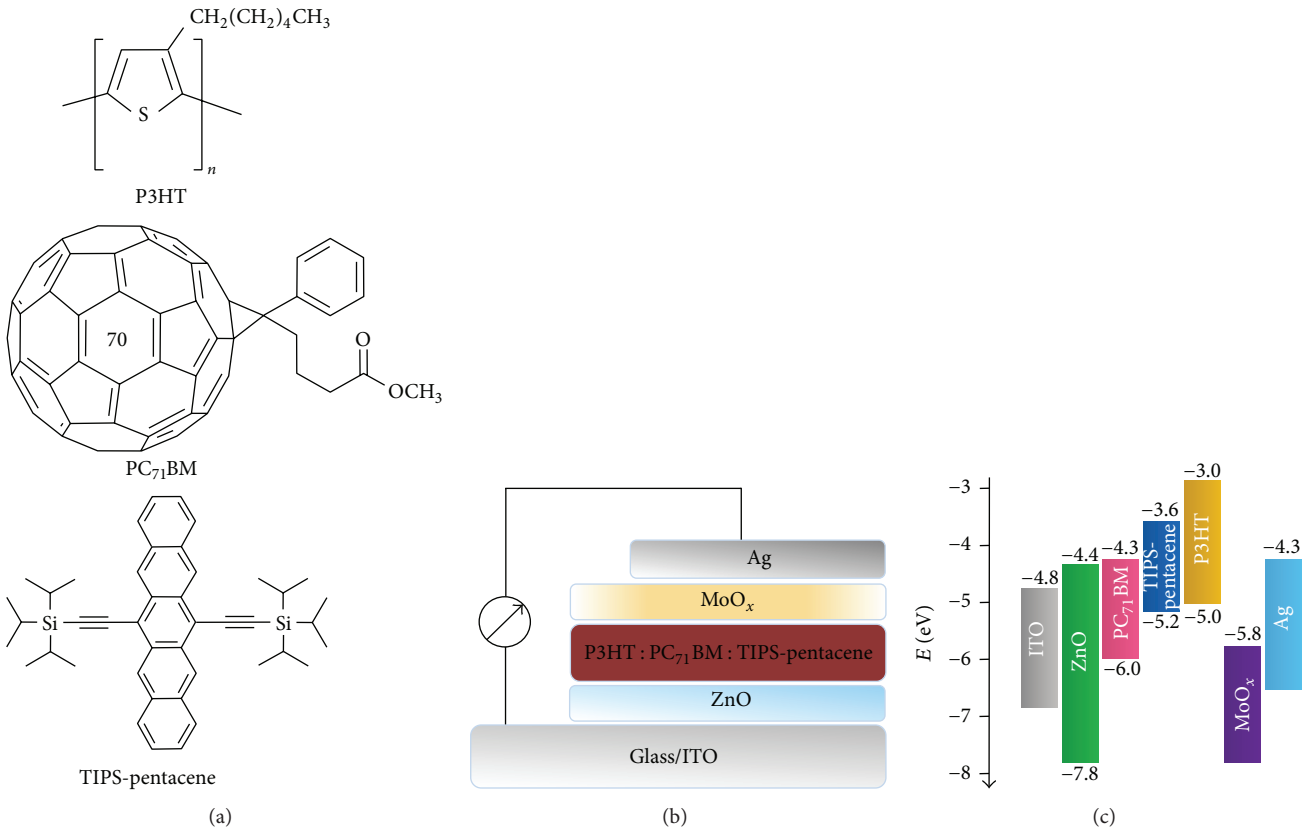

FIGURE 1: (a) Chemical structures of P3HT, $PC_{71}BM$, and TIPS-pentacene. (b) Schematic structure of PSCs in this work. (c) Energy band diagram of materials used in PSCs.

In this work, a high hole-mobility pentacene derivative of TIPS-pentacene (0.8 $cm^2V^{-1}s^{-1}$, which is nearly 4 folders as high as that of P3HT) [18, 19], with high solubility in organic solvents and deeper highest occupied molecular orbital (HOMO) of 5.20 eV compared with 5.00 eV of P3HT [20], was introduced in the P3HT : [6,6]-phenyl C71-butyric acid methyl ester ($PC_{71}BM$) blends. By adjusting the doping ratios of TIPS-pentacene from 0.3 to 1.2 wt%, the optimized PSC with 33% PCE improvement was obtained. The mechanism of TIPS-pentacene doping was elucidated through characterizing the morphology of active layers by X-ray diffraction (XRD) and atomic force microscopy (AFM). Furthermore, the variation of charge carrier mobility was investigated in the active layers from the hole-only and electron-only devices by using the space-charge-limited current (SCLC) method.

2. Experiment

The chemical structures of organic materials are shown in Figure 1(a), and the structure of PSCs is indium tin oxide (ITO)/ZnO (30 nm)/P3HT : $PC_{71}BM$: TIPS-pentacene (180 nm)/MoO_x (15 nm)/Ag (100 nm) as depicted in Figure 1(b). The ITO-coated glass substrates with a sheet resistance of 10 Ω/sq were consecutively in an ultrasonic bath containing detergent, acetone, deionized water, and isopropyl alcohol for 10 min each step and finally dried in an oven for 30 mins [21]. The ZnO precursor solution was spin-coated on the ITO-glass substrates. After baking at 200°C for 60 min in atmosphere, the substrates were transferred to a glove box (1 ppm O_2 and H_2O). P3HT (99.9%, Rieke Metals) and $PC_{71}BM$ (99.9%, Solarmer) were dissolved in 1,2-dichlorobenzene (DCB) and mixed in the glove box to obtain blend solutions (30 mg/mL) with a weight ratio of 1 : 1. TIPS-pentacene (99.9%, Rieke Metals) solution was separately prepared in DCB at a concentration of 2 mg/mL and then mixed with the blend solutions of P3HT : $PC_{71}BM$. TIPS-pentacene doping ratios in P3HT : $PC_{71}BM$ blends were adjusted from 0.3, 0.6, and 0.9 to 1.2 wt%. Then, P3HT : $PC_{71}BM$: TIPS-pentacene blend solutions were spin-coated on ZnO thin layer. After that, the substrates were solvent-annealed in a covered Petri dish for 20 mins and then were thermal-annealed at 120°C for 10 mins [22]. MoO_x (99.98%, Aldrich) layer was deposited onto the active layers at a rate of 1 to 3 Å/s at a pressure of 3.0×10^{-3} Pa in vacuum, followed by the deposition of Ag anode at a rate of 10 Å/s under a pressure of 3.0×10^{-3} Pa. The typical area of PSCs was 0.02 cm^2. All measurements were performed under ambient condition without encapsulation.

A light source integrated with a xenon lamp (CHF-XM35, Beijing Trust Tech) with an illumination power of 100 mW/cm^2 was used as a solar simulator. The curves under illumination and in the dark were measured with

Table 1: Comparison of device characteristics of P3HT : $PC_{71}BM$ PSCs with various TIPS-pentacene doping ratios.

Doping ratio (wt%)	V_{OC} (V)	J_{SC} (mA/cm^2)	FF (%)	PCE (%)	R_S (Ω·cm^2)	R_{SH} (Ω·cm^2)
Control	0.59 (±0.01)	9.63 (±0.14)	54.6 (±1.1)	3.10 (±0.22)	1.61 (±1.17)	290 (±36)
0.3	0.59 (±0.01)	10.05 (±0.19)	58.4 (±0.8)	3.46 (±0.15)	1.37 (±0.11)	561 (±58)
0.6	0.61 (±0.01)	10.86 (±0.17)	62.4 (±0.6)	4.13 (±0.12)	0.98 (±0.08)	708 (±67)
0.9	0.61 (±0.01)	10.31 (±0.21)	60.3 (±0.9)	3.79 (±0.17)	1.15 (±0.13)	689 (±57)
1.2	0.61 (±0.01)	8.95 (±0.22)	53.3 (±1.5)	2.91 (±0.26)	1.87 (±0.20)	348 (±41)

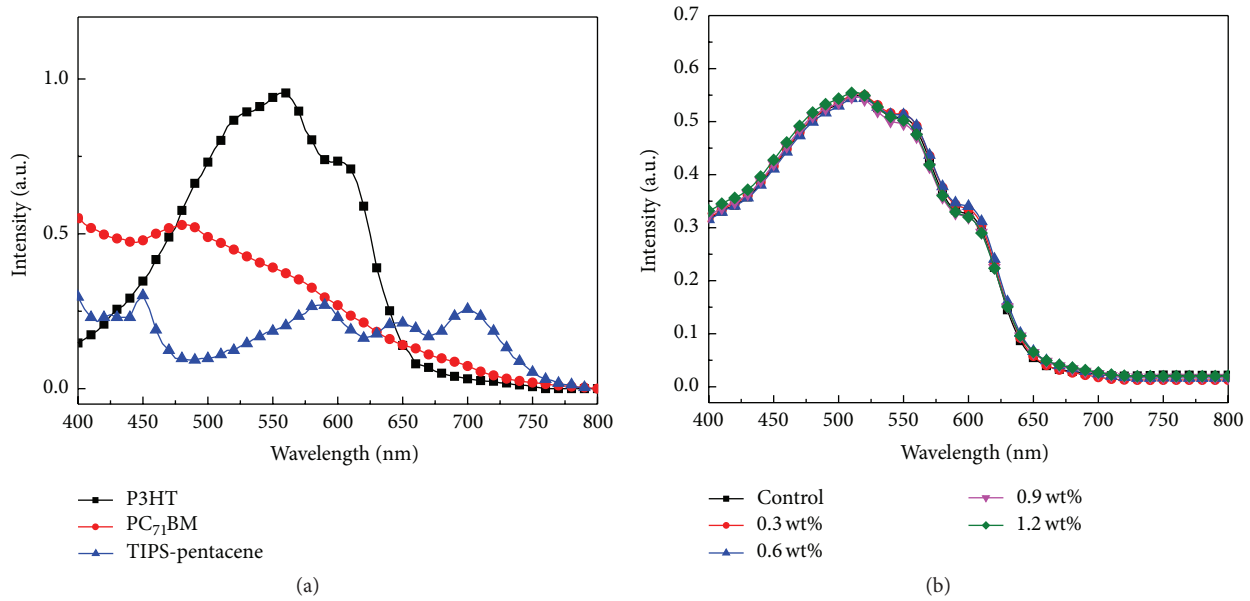

Figure 2: (a) Absorption spectra for thin films of P3HT, $PC_{71}BM$, and TIPS-pentacene. (b) Absorption spectra of P3HT : $PC_{71}BM$ active layers blended with various TIPS-pentacene doping ratios.

a Keithley 4200 programmable current-voltage source, and the external quantum efficiency (EQE) spectra were measured under the lump light passing through a monochromator. The ultraviolet-visible (UV-Vis) absorption spectra of the active layer on quartz substrates were measured using a Shimadzu UV1700 system. The film preparation condition for XRD (D1-HR XRD, Bede, Inc.) and AFM (MFP-3D-BIO, Asylum Research) measurement was kept the same as the device fabrication for comparison.

3. Results and Discussion

The absorption spectra of thin films of P3HT, $PC_{71}BM$, and TIPS-pentacene are shown in Figure 2(a). It can be seen that P3HT shows strong light absorption from 450 to 650 nm, while $PC_{71}BM$ has compensatory absorption from 350 to 550 nm. TIPS-pentacene exhibits a wide absorption in the visible region from 400 to 750 nm [20]. Figure 2(b) shows the absorption spectra of P3HT : $PC_{71}BM$ blend films with various TIPS-pentacene doping ratios. It is found that the absorption in the wavelength from 400 nm to 700 nm does not change significantly with the increase of TIPS-pentacene doping ratio. For the small amount of TIPS-pentacene, the absorption contribution of TIPS-pentacene is negligible. This phenomenon also indicates that the active layer thicknesses are unchanged with the doping of TIPS-pentacene.

The current density-voltage (J-V) characteristics of P3HT : $PC_{71}BM$ PSCs with various TIPS-pentacene doping ratios are displayed in Figure 3(a). The detailed parameters with error statistics including open circuit voltage (V_{OC}), J_{SC}, FF, and PCE are listed in Table 1. For the precise comparison of photovoltaic performance of PSCs with different TIPS-pentacene doping ratios, the relative change of the device parameters with increasing TIPS-pentacene doping ratios is summarized in Figure 3(b). The performance of pristine P3HT : $PC_{71}BM$ devices was chosen as the reference and set to 100%. All other devices data were normalized to that reference.

V_{OC} is 0.59 V for undoped devices and 0.3 wt% TIPS-pentacene doped devices and slightly increased to 0.61 V for the relative high TIPS-pentacene doping ratios devices. The increased V_{OC} is due to the multicharge separation phenomenon [23]. As shown in Figure 1(c), the HOMO of TIPS-pentacene is deeper than that of P3HT. After doping TIPS-pentacene, donor : donor : accepter blends were formed, and the additional TIPS-pentacene : $PC_{71}BM$ interface could facilitate the exciton separation in the bulk heterojunction. Even though little exciton can be formed on TIPS-pentacene for its negligible light absorption, the exciton can be formed

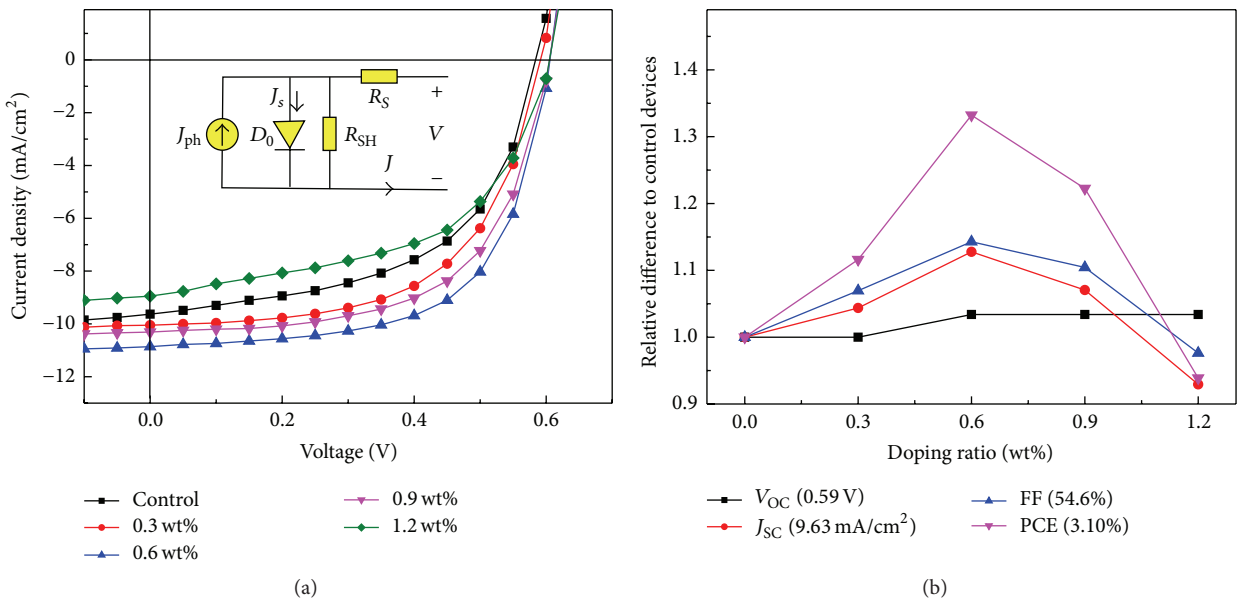

FIGURE 3: (a) J-V characteristics of P3HT : $PC_{71}BM$ PSCs with various TIPS-pentacene doping ratios. The inset shows the equivalent circuit model of PSC. (b) Relative change of the device parameters with increasing TIPS-pentacene doping ratios. The performance of pristine P3HT : $PC_{71}BM$ PSCs was chosen as reference and set to 100%. All other devices data were normalized to that reference.

on $PC_{71}BM$ for the obvious light absorption of $PC_{71}BM$. The exciton on $PC_{71}BM$ can be directly dissociated into free charge carrier by P3HT or TIPS-pentacene. V_{OC} of TIPS-pentacene doped PSCs is dependent on the composition of P3HT : $PC_{71}BM$ and TIPS-pentacene : $PC_{71}BM$ interfaces as reported by the previous works [24]. Thus, the additional TIPS-pentacene : $PC_{71}BM$ interface can affect the overall heterojunction energetics, resulting in the increased V_{OC}. With doping of TIPS-pentacene, a remarkable enhancement of J_{SC} and FF is observed. In the device doped with 0.3 wt% TIPS-pentacene, J_{SC} is increased to 10.05 mA/cm^2, and FF is increased to 58.4%. When doping 0.6% TIPS-pentacene, the device reaches its optimized performance with J_{SC} of 10.86 mA/cm^2, a FF of 62.4%, and a PCE of 4.13%. However, when the doping ratios are increased to 0.9% and 1.2%, the devices show decreased photovoltaic performance.

To further investigate the diode characteristics of PSCs, we modeled J-V characteristics with the Shockley diode equation as [25]

$$J = J_{ph} - J_s \left\{ \exp\left[\frac{V - JR_S A}{nkT/q} \right] - 1 \right\} - \frac{V - JR_S A}{R_{SH} A}, \quad (1)$$

where J_{ph} is the photocurrent, J_s is the reverse saturation current density, and n is the ideal factor. k is Boltzmann's constant, and T is the temperature. q is the electron charge, and A is the device area. The relevant diode parameters, including series resistance (R_S) and shunt resistance (R_{SH}), are summarized in Table 1. The decreased R_S and increased R_{SH} of PSC with 0.6 wt% TIPS-pentacene made a contribution to the enhanced J_{SC} and FF for efficient charge carrier transport and collection.

To illustrate the effect of molecular doping of TIPS-pentacene on J_{SC} of P3HT : $PC_{71}BM$ PSCs, EQE was employed. Figure 4 shows EQE spectra of P3HT : $PC_{71}BM$ PSCs with various TIPS-pentacene doping ratios in the wavelength ranging from 400 to 700 nm. The shape of EQE spectra resembles that of UV-Vis absorption spectra of the blend films. EQE values for devices exceed 50% in the region of 400–570 nm. It is found that the largest EQE of 68.9% is obtained for PSCs with 0.6 wt% TIPS-pentacene doped. However, when the doping ratios of TIPS-pentacene in P3HT : $PC_{71}BM$ blends were further increased, EQE of PSCs was decreased.

To further investigate EQE variation, the theoretical J_{SC} values ($J_{SC(EQE)}$) are obtained via integrating EQE. The formula of integration is presented as

$$J_{SC(EQE)} = \int \frac{q\lambda}{hc} \mathrm{EQE}(\lambda)\, S(\lambda)\, d\lambda, \quad (2)$$

where $S(\lambda)$ is AM1.5 solar spectral density.

The inset of Figure 4 shows $J_{SC(EQE)}$ of PSCs with various TIPS-pentacene doping ratios. All $J_{SC(EQE)}$ are about 1.31 mA/cm^2 less than the measured values in J-V curves, as the offered EQE spectra lack the part less than 400 nm. $J_{SC(EQE)}$ is increased from 7.76 mA/cm^2 for undoped devices to 9.23 mA/cm^2 for 0.6 wt% TIPS-pentacene doped devices and then decreased to 7.61 mA/cm^2 for 1.2 wt% TIPS-pentacene doped devices. This situation is similar to the characteristics of J_{SC} as listed in Table 1.

The effect of different TIPS-pentacene doping ratios in P3HT : $PC_{71}BM$ blends on the charge carrier transport properties was further investigated by using SCLC model. The hole-only devices with a configuration of ITO/MoO_x (15 nm)/P3HT : $PC_{71}BM$: TIPS-pentacene (180 nm)/MoO_x (15 nm)/Ag (100 nm) and electron-only devices with

Table 2: The hole mobility and electron mobility of the hole-only and electron-only devices with various TIPS-pentacene doping ratios.

Doping ratio (wt%)	μ_h ($cm^2V^{-1}s^{-1}$)	μ_e ($cm^2V^{-1}s^{-1}$)	μ_h/μ_e
Control	1.3×10^{-4}	2.8×10^{-4}	0.46
0.3	1.7×10^{-4}	2.7×10^{-4}	0.63
0.6	2.6×10^{-4}	2.6×10^{-4}	1.00
0.9	2.0×10^{-4}	2.4×10^{-4}	0.83
1.2	9.5×10^{-5}	2.0×10^{-4}	0.48

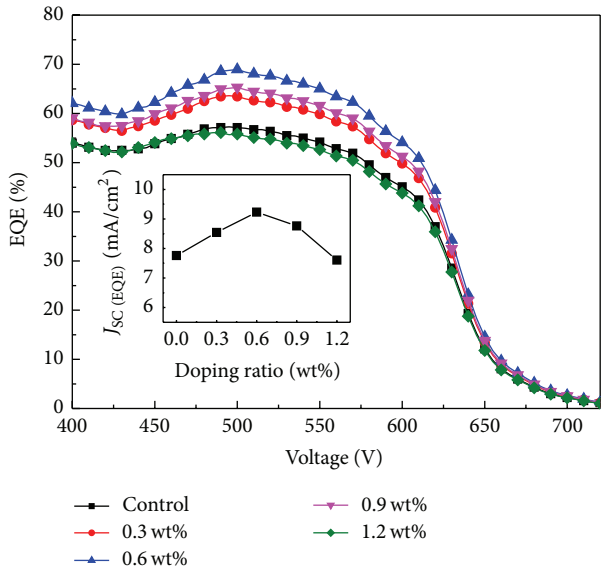

Figure 4: EQE spectra of P3HT : $PC_{71}BM$ PSCs with various TIPS-pentacene doping ratios. The inset shows the integral J_{SC} of PSCs with various TIPS-pentacene doping ratios.

a configuration of ITO/ZnO (30 nm)/P3HT : $PC_{71}BM$: TIPS-pentacene (180 nm)/Bphen (5 nm)/Ag (100 nm) were fabricated, respectively. The hole mobility in the hole-only devices and the electron mobility in the electron-only devices can be calculated using Mott-Gurney law as

$$J = \frac{9}{8}\varepsilon\varepsilon_0\mu\frac{V^2}{d^3}, \quad (3)$$

where μ is the charge carrier mobility. ε is the relative permittivity of polymer assumed to be 3, and ε_0 is the vacuum dielectric constant of 8.85×10^{-12} F/m. V is the voltage, and d is the thickness of the layer.

J-V characteristics of the hole-only and electron-only devices with various TIPS-pentacene doping ratios in P3HT : $PC_{71}BM$ blends are presented in Figures 5(a) and 5(b), respectively. The hole mobility and the electron mobility of corresponding devices are listed in Table 2. In the hole-only devices, the hole mobility of undoped P3HT : $PC_{71}BM$ device was 1.3×10^{-4} $cm^2V^{-1}s^{-1}$. After doping TIPS-pentacene, hole mobilities of the devices were calculated to be 1.7×10^{-4}, 2.6×10^{-4}, 2.0×10^{-4}, and 9.5×10^{-5} $cm^2V^{-1}s^{-1}$ for 0.3 wt%, 0.6 wt%, 0.9 wt%, and 1.2 wt% doping ratios. On the other hand, in the electron-only devices, the electron mobility is slightly decreased with the increase of TIPS-pentacene doping ratio in P3HT : $PC_{71}BM$: TIPS-pentacene blends. In particular, balanced charge carrier mobility of 1.00 was obtained in the active layer with 0.6 wt% TIPS-pentacene, which ensures efficient charge transport and collection in P3HT : $PC_{71}BM$: TIPS-pentacene blends, resulting in the enhancement of both J_{SC} and FF. However, when TIPS-pentacene doping ratios are high, PCE is decreased. The degraded performances are due to the decreased hole mobilities, leading to an unbalance charge transport in P3HT : $PC_{71}BM$: TIPS-pentacene blends. In this condition, hole with lower mobility induced cumulative charge carriers in the active layer due to the SCLC effect [26]. Therefore, PCE of PSCs with high TIPS-pentacene doping ratios is decreased by the reduction of J_{SC} and FF.

To demonstrate TIPS-pentacene doping effect on the crystallinity of P3HT, P3HT : $PC_{71}BM$ blends without and with 0.6 wt% TIPS-pentacene were characterized by XRD as shown in Figure 6. XRD spectra show obvious α-axis orientation of P3HT crystallite at a peak of 2θ near 5.4°, corresponding to the (100) crystal plane [21]. Compared with P3HT : $PC_{71}BM$ blends, the 0.6 wt% TIPS-pentacene doped P3HT : $PC_{71}BM$ exhibits higher (100) peak. This result indicated that the enhancement of hole mobility for TIPS-pentacene doped blends could result from the crystallinity enhancement of P3HT.

To further investigate the effect of molecular doping of TIPS-pentacene on the morphology of P3HT : $PC_{71}BM$ blends, the surface morphology of P3HT : $PC_{71}BM$ blends and 0.6 wt% TIPS-pentacene doped P3HT : $PC_{71}BM$ blends was examined by using AFM as shown in Figure 7. For P3HT : $PC_{71}BM$ blends, the root-mean-square (RMS) roughness is 6.14 nm. The rough texture suggests that the enhancement of ordered structure is due to the self-organization of thick P3HT : $PC_{71}BM$ blends during slow growing process. After doping 0.6 wt% TIPS-pentacene, RMS increases slightly to 6.28 nm. It has been reported that the increased RMS of P3HT : $PC_{71}BM$ blends demonstrated that P3HT had enhanced crystallinity [22]. Based on this phenomenon, it could also be deducted that the crystallinity of P3HT in the active layer was improved with the molecular doping of TIPS-pentacene, which is consistent with the results of XRD measurement mentioned above. In addition, the rough surface could shorten the charge-transport distance from P3HT : $PC_{71}BM$ blends to Ag anode, resulting in an efficient hole collection. AFM phase images of P3HT : $PC_{71}BM$ blends and 0.6 wt% TIPS-pentacene doped P3HT : $PC_{71}BM$ blends are presented in Figures 7(c) and 7(d). It can be seen from the two phase images that no obvious ternary TIPS-pentacene domain was observed, indicating that small doping ratio would not change P3HT : $PC_{71}BM$ interpenetrating network.

4. Conclusion

In summary, the solution-processed P3HT : $PC_{71}BM$: TIPS-pentacene PSCs with 0, 0.3, 0.6, 0.9, and 1.2 wt% TIPS-pentacene doping ratios were fabricated. 0.6 wt% TIPS-pentacene doped PSC exhibited an enhanced J_{SC} and FF,

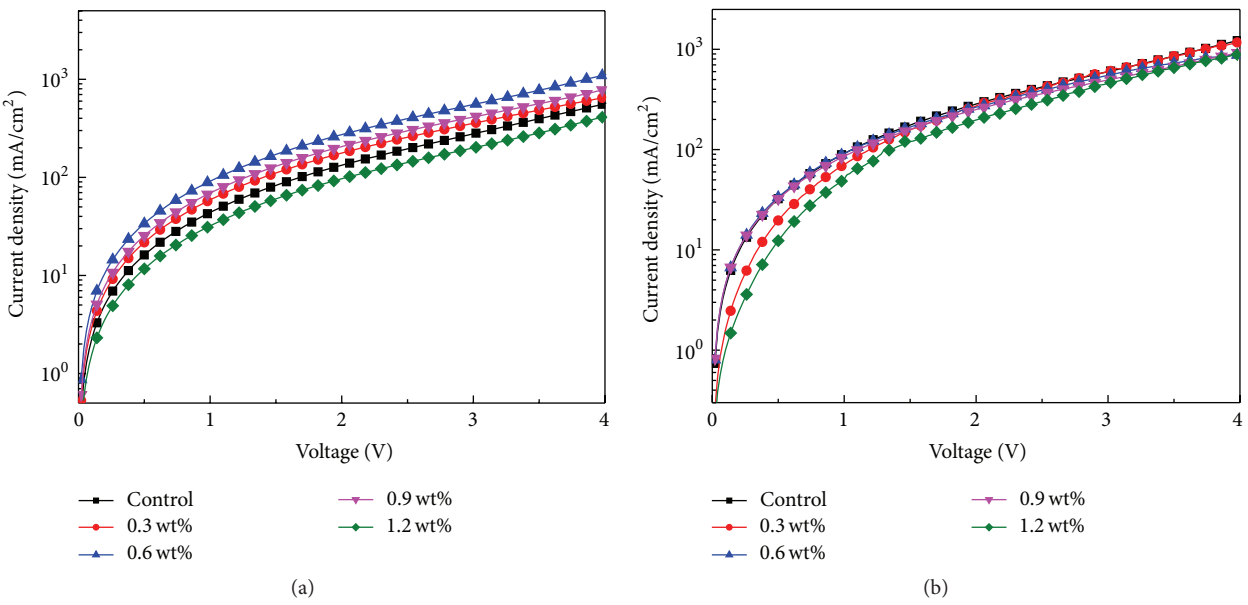

FIGURE 5: J-V characteristics of (a) hole-only and (b) electron-only devices.

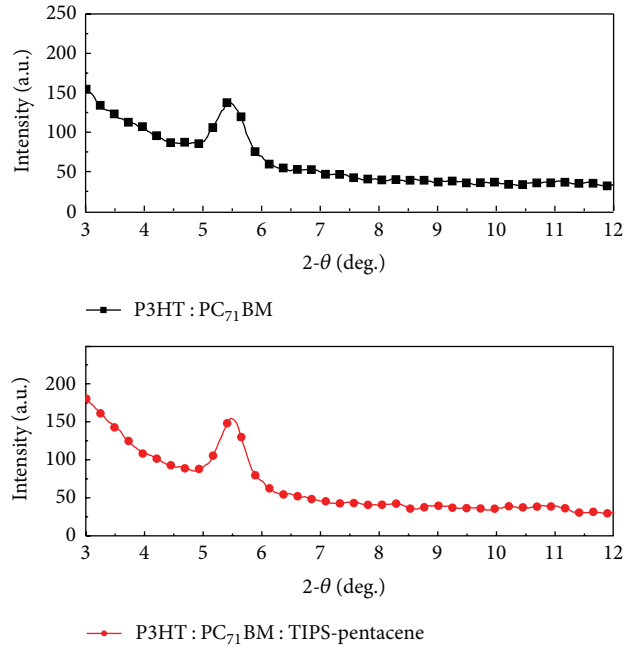

FIGURE 6: XRD spectra of P3HT : PC$_{71}$BM blends without and with 0.6 wt% TIPS-pentacene.

resulting in a maximum PCE of 4.13%, which is 33% higher compared with the undoped PSC. The improved photovoltaic performance was originated from the balanced charge carrier mobility, enhanced crystallinity, and matched cascade energy level alignment in P3HT : PC$_{71}$BM : TIPS-pentacene blends, resulting in efficient charge separation, transport, and collection. This work can significantly enhance our understanding of the mechanism of molecular doping with high-mobility small organic molecules on the photovoltaic performance of PSCs.

Conflict of Interests

The authors declare that there is no conflict of interests regarding the publication of this paper.

Acknowledgments

This research was funded by the Foundation of the National Natural Science Foundation of China (NSFC) (Grant no.

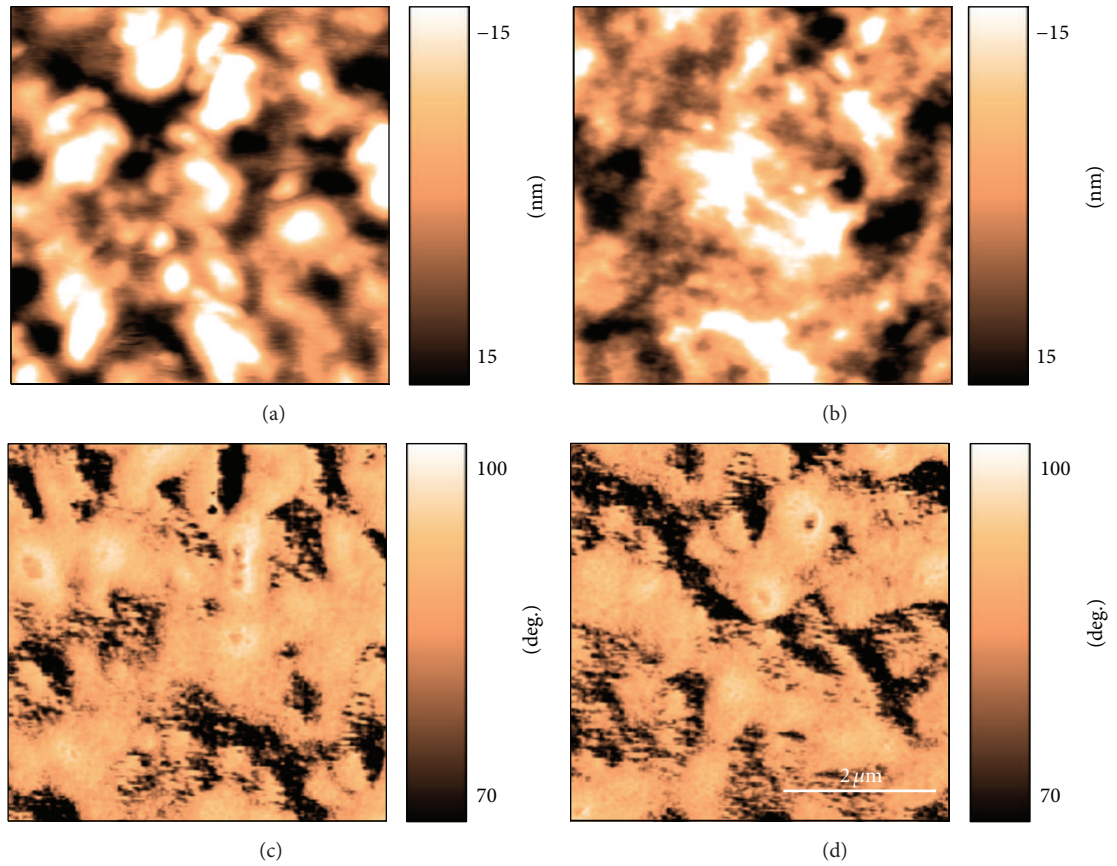

FIGURE 7: AFM morphology images of (a) P3HT : $PC_{71}BM$ blend film and (b) P3HT : $PC_{71}BM$ with a 0.6 wt% TIPS-pentacene doping ratio blend film. Corresponding AFM phase images ((c) and (d)) are shown below each respective morphology image. Image size is 5 μm × 5 μm.

61177032) and the National Science Funds for Creative Research Groups of China (Grant no. 61421002).

References

[1] A. J. Heeger, "25th anniversary article: bulk heterojunction solar cells: understanding the mechanism of operation," *Advanced Materials*, vol. 26, no. 1, pp. 10–28, 2014.

[2] V. Vohra, K. Kawashima, T. Kakara et al., "Efficient inverted polymer solar cells employing favourable molecular orientation," *Nature Photonics*, vol. 9, no. 6, pp. 403–408, 2015.

[3] J. Yu, Y. Zheng, and J. Huang, "Towards high performance organic photovoltaic cells: a review of recent development in organic photovoltaics," *Polymers*, vol. 6, no. 9, pp. 2473–2509, 2014.

[4] P.-T. Huang, Y.-H. Chen, B.-Y. Lin, and W.-P. Chuang, "Homogenized poly(3-hexylthiophene)/methanofullerene film by addition of end-functionalized compatibilizer and its application to polymer solar cells," *International Journal of Photoenergy*, vol. 2015, Article ID 762532, 7 pages, 2015.

[5] A. Iwan, B. Boharewicz, I. Tazbir, A. Sikora, and B. Zboromirska-Wnukiewicz, "Silver nanoparticles in PEDOT:PSS layer for polymer solar cell application," *International Journal of Photoenergy*, vol. 2015, Article ID 764938, 9 pages, 2015.

[6] J.-D. Chen, C. Cui, Y.-Q. Li et al., "Single-junction polymer solar cells exceeding 10% power conversion efficiency," *Advanced Materials*, vol. 27, no. 6, pp. 1035–1041, 2015.

[7] C.-C. Chen, W.-H. Chang, K. Yoshimura et al., "An efficient triple-junction polymer solar cell having a power conversion efficiency exceeding 11%," *Advanced Materials*, vol. 26, no. 32, pp. 5670–5677, 2014.

[8] L. Dou, J. You, Z. Hong et al., "25th anniversary article: a decade of organic/polymeric photovoltaic research," *Advanced Materials*, vol. 25, no. 46, pp. 6642–6671, 2013.

[9] X. G. Guo, N. J. Zhou, S. J. Lou et al., "Polymer solar cells with enhanced fill factors," *Nature Photonics*, vol. 7, no. 10, pp. 825–833, 2013.

[10] N. Wang, J. Yu, Y. Zheng, Z. Guan, and Y. Jiang, "Organic photovoltaic cells based on a medium-bandgap phosphorescent material and C60," *The Journal of Physical Chemistry C*, vol. 116, no. 9, pp. 5887–5891, 2012.

[11] L. Ye, S. Zhang, W. Ma et al., "From binary to ternary solvent: morphology fine-tuning of D/A blends in PDPP3T-based polymer solar cells," *Advanced Materials*, vol. 24, no. 47, pp. 6335–6341, 2012.

[12] Y. Liang, Z. Xu, J. Xia et al., "For the bright future-bulk heterojunction polymer solar cells with power conversion efficiency of 7.4%," *Advanced Materials*, vol. 22, no. 20, pp. E135–E138, 2010.

[13] S. Liu, P. You, J. Li et al., "Enhanced efficiency of polymer solar cells by adding a high-mobility conjugated polymer," *Energy & Environmental Science*, vol. 8, no. 5, pp. 1463–1470, 2015.

[14] Y. Zhang, H. Zhou, J. Seifter et al., "Molecular doping enhances photoconductivity in polymer bulk heterojunction solar cells," *Advanced Materials*, vol. 25, no. 48, pp. 7038–7044, 2013.

[15] C.-T. Lee and C.-H. Lee, "Conversion efficiency improvement mechanisms of polymer solar cells by balance electron-hole mobility using blended P3HT:PCBM:pentacene active layer," *Organic Electronics*, vol. 14, no. 8, pp. 2046–2050, 2013.

[16] H.-Y. Lee and H.-L. Huang, "Investigation performance and mechanisms of inverted polymer solar cells by pentacene doped P3HT: PCBM," *International Journal of Photoenergy*, vol. 2014, Article ID 812643, 9 pages, 2014.

[17] H. Du, Z. Deng, J. Lun et al., "Pentacene doping for the efficiency improvement of polymer solar cells," *Synthetic Metals*, vol. 161, no. 19-20, pp. 2083–2086, 2011.

[18] G. Giri, E. Verploegen, S. C. B. Mannsfeld et al., "Tuning charge transport in solution-sheared organic semiconductors using lattice strain," *Nature*, vol. 480, no. 7378, pp. 504–508, 2011.

[19] R. Mauer, M. Kastler, and F. Laquai, "The impact of polymer regioregularity on charge transport and efficiency of P3HT:PCBM photovoltaic devices," *Advanced Functional Materials*, vol. 20, no. 13, pp. 2085–2092, 2010.

[20] R. J. Davis, M. T. Lloyd, S. R. Ferreira et al., "Determination of energy level alignment at interfaces of hybrid and organic solar cells under ambient environment," *Journal of Materials Chemistry*, vol. 21, no. 6, pp. 1721–1729, 2011.

[21] W. Ma, C. Yang, X. Gong, K. Lee, and A. J. Heeger, "Thermally stable, efficient polymer solar cells with nanoscale control of the interpenetrating network morphology," *Advanced Functional Materials*, vol. 15, no. 10, pp. 1617–1622, 2005.

[22] M. Reyes-Reyes, K. Kim, and D. L. Carroll, "High-efficiency photovoltaic devices based on annealed poly(3-hexylthiophene) and 1-(3-methoxycarbonyl)-propyl-1-phenyl-(6,6) C61 blends," *Applied Physics Letters*, vol. 87, no. 8, Article ID 083506, 2005.

[23] J. Huang, J. Yu, Z. Guan, and Y. Jiang, "Improvement in open circuit voltage of organic solar cells by inserting a thin phosphorescent iridium complex layer," *Applied Physics Letters*, vol. 97, no. 14, Article ID 143301, 3 pages, 2010.

[24] P. P. Khlyabich, B. Burkhart, and B. C. Thompson, "Compositional dependence of the open-circuit voltage in ternary blend bulk heterojunction solar cells based on two donor polymers," *Journal of the American Chemical Society*, vol. 134, no. 22, pp. 9074–9077, 2012.

[25] K. Bouzidi, M. Chegaar, and A. Bouhemadou, "Solar cells parameters evaluation considering the series and shunt resistance," *Solar Energy Materials and Solar Cells*, vol. 91, no. 18, pp. 1647–1651, 2007.

[26] C. Melzer, E. J. Koop, V. D. Mihailetchi, and P. W. M. Blom, "Hole transport in poly(phenylene vinylene)/methanofullerene bulk-heterojunction solar cells," *Advanced Functional Materials*, vol. 14, no. 9, pp. 865–870, 2004.